Development 140, 3275-3284 (2013) doi:10.1242/dev.096057

TIE-DYE: a combinatorial marking system to visualize and genetically manipulate clones during development in *Drosophila melanogaster*

Melanie I. Worley, Linda Setiawan and Iswar K. Hariharan*

SUMMARY

Two types of information are particularly valuable in understanding the development of a tissue or an organ from a small population of founder cells. First, it is useful to know the composition of the final structure in terms the contribution of individual founder cells. Second, it is important to understand cell-cell interactions. To facilitate the study of both of these aspects of organ development at a tissue-wide level, we have developed a method, TIE-DYE, that allows simultaneous lineage tracing of multiple cell populations as well as the genetic manipulation of a subset of these populations. Seven uniquely marked categories of cells are produced by site-directed recombination of three independent cassettes. We have used the TIE-DYE method to estimate the number of founder cells that give rise to the wing-imaginal disc during normal development and following compensatory growth caused by X-ray irradiation of the founder cells. We also show that four out of the seven types of marked clones can be genetically manipulated by gene overexpression or RNAi knockdown, allowing an assessment of the consequences of these manipulations on the entire wing disc. We demonstrate the utility of this system in studying the consequences of alterations in growth, patterning and cell-cell affinity.

KEY WORDS: Multicolor lineage technique, Imaginal disc, *Drosophila*

INTRODUCTION

During the development of an organism, the fate of cells is regulated by both lineage and extracellular signals. Thus, to understand the development of a tissue or an organ there is a need to describe the origin of cells as well as interactions between cells. Additionally, there are modes of regulation affecting organ size determination and tissue homeostasis that can only be appreciated by studying the tissue as a whole rather than by examining the properties of individual cells. Studying these phenomena would be greatly aided by methods that enable tracking the lineage of many cells within an organ and at the same time examining the consequences of local perturbations on the tissue as a whole.

Experiments to track cell lineages during development have been performed in many different ways (reviewed by Kretzschmar and Watt, 2012), including the study of gynandromorphs (Sturtevant, 1929; Garcia-Bellido and Merriam, 1969), by using chimeric embryos (Le Douarin and Barq, 1969), and by injecting dyes or enzymes into individual cells in order to label their progeny (Weisblat et al., 1978). More recently, genetic systems that stochastically label cells and all of their progeny have been used to study cell lineages. In addition, by combining systems that direct site-specific recombination with genes encoding multiple fluorescent proteins, it has become possible to label multiple lineages uniquely in a tissue simultaneously as was achieved with the Brainbow system (Livet et al., 2007) in the mouse nervous system. This sparked the creation of multicolor labeling systems in other model organisms, which have been used to map multiple single cell projections in the nervous system (Livet et al., 2007; Hadjieconomou et al., 2011; Hampel et al., 2011; Boulina et al., 2013) to track developmental lineages in the zebrafish heart (Gupta and Poss, 2012) and to visualize stem cell-based replacement during homeostasis of the mouse gut (Snippert et al., 2010). The use of these systems demonstrates that being able to simultaneously and uniquely label many cells or follow multiple cell lineages at once can lead to novel scientific discoveries.

The study of *Drosophila* development has led to many important findings about the genetic regulation of pattern formation. A key experimental approach has been to express a variety of genes with the GAL4/UAS binary system (Fischer et al., 1988; Brand and Perrimon, 1993). Both dBrainbow and Flybow (Hadjieconomou et al., 2011; Hampel et al., 2011) use the GAL4/UAS system for multicolor-labeling of cells and cell lineages in *Drosophila*. This is achieved by stochastic site-specific recombination to place one of several genes encoding fluorescent proteins downstream of a GAL4-responsive promoter in a restricted subset of the marked clones. In addition, these systems only permanently mark cell lineages if the source of GAL4 is ubiquitously expressed (reviewed by del Valle Rodríguez et al., 2012).

Several methods have been developed to manipulate either the genotype or gene expression within clones of cells. In *Drosophila*, this can be achieved efficiently either by FLP/FRT-mediated mitotic recombination that efficiently generates patches of mutant cells and wild-type sister clones (Golic, 1991; Xu and Rubin, 1993), or by the FLP-out method where FLP/FRT-mediated excision of a STOP cassette upstream of GAL4, results in heritable GAL4 expression (Pignoni and Zipursky, 1997). Systems using mitotic recombination have been further refined by positively marking the GAL4-expressing clones or by marking both sister clones following the recombination (Lee et al., 2000; Griffin et al., 2009; Yu et al., 2009). However, in all of these cases, most of the remaining cells in the tissue are not labeled and hence it is not easy to infer the consequence of generating a patch of mutant cells on the remainder of the organ.

Department of Molecular and Cell Biology, University of California, Berkeley, Berkeley, CA 94720-3200, USA.

*Author for correspondence (ikh@berkeley.edu)

Accepted 15 May 2013

Recently developed heterologous systems, such as the Q-system (Potter et al., 2010) and the lex-GAD system (Szüts and Bienz, 2000; Lai and Lee, 2006; Yagi et al., 2010), could potentially be used together with GAL4/UAS-based methods of multicolor cell labeling, such as dBrainbow and Flybow, so as to combine lineage tracing with gene manipulations in subsets of cells. However, most current collections of transgenic lines that express RNAi constructs or cDNAs are UAS driven and thus their expression cannot be directed by these newer heterologous systems. Here, we describe a way to combine simultaneous multicolor lineage analysis with overexpression or knockdown of UAS-regulated constructs in a subset of the marked clones. We have used this system, first as a method of lineage tracing, to assess the number of founder cells in the wing-imaginal discs under conditions of normal development and compensatory proliferation following X-ray irradiation. We then demonstrate its utility in examining the effects of manipulating genes that regulate cell proliferation or patterning and its applicability to study phenomena that can involve multiple clones of cells, such as the sorting of cells from epithelia.

MATERIALS AND METHODS

Drosophila stocks and transgenes

All *Drosophila* stocks, unless otherwise mentioned, were obtained from the Bloomington Stock Center. The TIE-DYE marking system was generated by the recombination of the following transgenes: *Act <stop <lacZ-NLS* (Struhl and Basler, 1993) and *Ubi <stop <eGFP-NLS* (Evans et al., 2009) onto the same 2nd chromosome; and *Act <stop <GAL4* (Pignoni and Zipursky, 1997) and *UAS-His2A::mRFP* (Emery et al., 2005) onto the same 3rd chromosome. A stock containing these recombinant chromosomes was built, along with a stock with *hsFLP* to facilitate testing UAS-driven transgenes. Although this stock with *hsFLP* can be maintained successfully for multiple generations, at room temperature, germ-line FLP-out clones are sometimes observed where all cells in the progeny are labeled with a given marker. The stock is therefore re-assembled using the following stocks: *y, w, hsFLP; Sp; Dr / SM5-TM6B* and *w; Act <stop <lacZ^{nls}, Ubi <stop <GFP^{nls}; Act <stop <GAL4, UAS-his2A::RFP / SM5-TM6B*.

Experimental animals were generated by the following crosses: (1) *y, w, hsFLP × w; ubi <stop <GFP^{nls}, act5C <stop <lacZ^{nls}; Act5C <stop <GAL4, UAS-his2A::RFP / SM5-TM6B*; or for experiments with an additional UAS-transgene, (2) *y, w, hsFLP; ubi <stop <GFP^{nls}, act5C <stop <lacZ^{nls}; Act5C <stop <GAL4, UAS-his2A::RFP / SM5-TM6B × UAS-X*. The following transgenes were used for overexpression experiments: *UAS-ci.3m.HA* (Price and Kalderon, 1999), *UAS-dpp.S 42B.4* (Staehling-Hampton and Hoffmann, 1994), *UAS-Ras85D.V12* (Lee et al., 1996) and *UAS-yki.S168A.V5* (Oh and Irvine, 2009). The following transgenes were used for RNAi knockdown experiments and included *UAS-DCR2*: *ci^{RNAi}=TRiP.JF07715, ex^{RNAi}=TRiP.JF03120, Myc^{RNAi}* (VDRC), *y^{RNAi}* (VDRC) and *yki^{RNAi}=TRIPJF03119*.

Immunohistochemistry and image processing

Larvae were dissected in PBS and fixed in 4% paraformaldehyde for 15 minutes at room temperature. Primary antibodies used were either rabbit anti-β-galactosidase (1:500; MP Biomedicals) or mouse anti-β-galactosidase (1:500; Promega), with ALEXA Fluor-633 (anti-rabbit or anti-mouse; 1:1000; Invitrogen) as secondary antibodies. Tissues were mounted in SlowFade Gold Antifade (Life Technologies). Fluorescent images were taken on a Leica TCS SL confocal microscope with Ar (488 λ), GreNe (543 λ) and HeNe (633 λ) lasers using 16× and 40× objectives. No additional stain was performed to detect the GFP or RFP in the tissues. Images of GAL4(+) and GAL4(–) clones were generated using Adobe Photoshop CS3; the selection tool was used to select areas above a cut-off threshold in the red channel to generate images of both RFP(+)-only clones and non-RFP(+) clones (by subtraction).

TIE-DYE clone generation

Clones were induced by heat shocks in a 37°C circulating water bath, in either vials or on grape-juice plates (placed in a secondary container). For experiments conducted on grape-juice plates, L1 larvae were picked ~24 hours after egg lay (AEL) and placed in a vial with yeast paste. The durations of the heat-shocks were experimentally determined for different developmental stages. A heat-shock of 30 minutes was used for embryos and 15 minutes was used for early/late-stage larvae to generate a high clone frequency with diverse clone types. Twenty-four-hour egg collections (in vials) were conducted for experiments in Figs 4-6, clones were induced during 2nd/3rd instar and discs were dissected as late 3rd instar larvae.

Embryo collection and X-ray irradiation

Eggs were collected on grape-juice plates with yeast paste for 2 hours at 25°C, after a 30-minute pre-collection. At 16±1 hours AEL, embryos were heat-shocked for 30 minutes and then exposed to X-rays generated from a Faxitron TRX5200 operating at 125 V and 3.0 mA. The irradiated samples were placed at a distance of 40.3 cm from the X-ray source on a micro-go-round and weight block, producing an exposure rate of ~3.2 Gy/minute. Third instar larvae were dissected at 96-120 hours AEL. The animals that received the highest dose of X-ray irradiation showed the most delay in development, as previously described (Hussey et al., 1927; Halme et al., 2010).

Imaginal disc fragmentation and transplantation

Wing discs were fragmented and transplanted into an adult female host, as described previously (Bosch et al., 2005). Following the induction of TIE-DYE clones, the mid-3rd instar larvae were sterilized (1 minute in 50% bleach) and dissected. Fragments of the ventral wing disc were removed with tungsten needles, and the resulting three-quarter disc fragments were injected into the abdomen of Oregon-R adult females that were kept at 25°C. Imaginal discs were recovered from hosts after 4 days and stained.

Clone area tracing and statistical analysis

Tracing of the merged images was performed using Adobe Photoshop CS3 Smart Highlighting Tool to follow boundaries of clones. The different channels were visualized independently to determine the number of different markers present in a clone and therefore the appropriate color. The clone area tracings were used to measure the clone area with the Adobe Photoshop CS3 Analysis Record Measurement tool and the particular marker combinations present in the tissue. Statistical analysis of the clone area data was performed using GraphPad Prism (version 4). For comparing GAL4(+) with GAL4(–) clone areas for *expanded^{RNAi}* (supplementary material Fig. S4), we used the Mann-Whitney, two-tailed statistical test. For comparing the proportion of GAL4(+) cells between multiple genotypes, we used a one-way ANOVA test with Dunnett's multiple comparison test between the control and other genotypes.

Generation of model for number of founder cells

The recombination frequency of the three-different FLP-out constructs was estimated by measuring the area of each marker versus the total area (using clone area tracings) from control wing discs. The recombination frequency depends on the duration of heat-shock. The probability of any color event was calculated from these measured recombination frequencies by using the following equations.

Red: $pR=P(GAL4)\times(1-P(GFP))\times(1-P(lacZ))$

Green: $pG=P(GFP)\times(1-P(GAL4))\times(1-P(lacZ))$

Blue: $pB=P(lacZ)\times(1-P(GAL4))\times(1-P(GFP))$

Yellow: $pY=P(GAL4)\times P(GFP)\times(1-P(lacZ))$

Purple: $pP=P(GAL4)\times P(lacZ)\times(1-P(GFP))$

Teal: $pT=P(GFP)\times P(lacZ)\times(1-P(GAL4))$

White: $pW=P(GFP)\times P(GAL4)\times P(lacZ)$

Black: $pX=(1-P(GFP))\times(1-P(GAL4))\times(1-P(lacZ))$

With these probabilities of each color, the probability of any given event (such as 2 blue, 3 red, 2 green, 1 yellow, 1 teal, 0 purple, 0 white and 1 black founder cells) was calculated using the multinomial formula:

$$P = \frac{(\mathbf{r}+\mathbf{g}+\mathbf{b}+\mathbf{y}+\mathbf{p}+\mathbf{t}+\mathbf{w}+\mathbf{x})!}{\mathbf{r}!\times\mathbf{g}!\times\mathbf{b}!\times\mathbf{y}!\times\mathbf{p}!\times\mathbf{t}!\times\mathbf{w}!\times\mathbf{x}!} \times(\boldsymbol{pR}^{\mathbf{r}}\times\boldsymbol{pG}^{\mathbf{g}}\times\boldsymbol{pB}^{\mathbf{b}}\times\boldsymbol{pY}^{\mathbf{y}}\times\boldsymbol{pP}^{\mathbf{p}}\times\boldsymbol{pT}^{\mathbf{t}}\times\boldsymbol{pW}^{\mathbf{w}}\times\boldsymbol{pX}^{\mathbf{x}})$$

r, g, b, y, p, t, w, x=number of red, green, blue, yellow, purple, teal, white and black founder cells.

The probabilities of all possible situations from 1 to 40 founder cells were calculated using a python script and then the probabilities were grouped in one of two ways: (1) the total number of colors represented (one through eight) or (2) specific color outcomes (such as all ways to generate a tissue with only green, yellow and teal marked cells present). From an experimental outcome, we calculated the probability that the disc was generated from 1 to 20 founder cells (i.e. a disc with only red, yellow, purple and white cells was calculated to have the highest probability of being from five founder cells; shown in Fig. 2N).

RESULTS

To visualize the clonal composition of a tissue as well as interactions between mutant cells and wild-type cells throughout the tissue, we developed a system we have named TIE-DYE that generates seven distinct populations of irreversibly marked clones in an unlabeled background. In addition, four out of the seven classes of clones are GAL4 dependent (see below). This allows co-expression of additional transgenes, to manipulate gene function, in a subset of the marked clones, while adjacent clones remain wild type.

The TIE-DYE system takes advantage of the stochastic nature of FLP-induced recombination to excise transcriptional stop-cassettes upstream of *lacZ* (Struhl and Basler, 1993), *GFP* (Evans et al., 2009) and/or *GAL4* (Pignoni and Zipursky, 1997), such that, following recombination, expression is sustained in that cell and all of its descendants (Fig. 1A). As a result, cells can potentially activate the expression of any one, any combination of two, or all three FLP-out genes, thus generating seven possible combinations, along with an unmarked population (Fig. 1B). Because, unlike the classical dye-injection experiments, the marking of cells is achieved using three independent excisions, we have named the system TIE-DYE. Two of the FLP-out constructs drive marker expression directly and are therefore GAL4 independent. The third FLP-out construct activates the expression of GAL4, which promotes expression of the third marker, *UAS-his2A::RFP*. Thus, TIE-DYE allows concurrent GAL4-driven overexpression or RNAi knockdown in the RFP-expressing subpopulation. A heat-shock promoter controls the expression of FLP and therefore the duration of a heat-shock affects both the number and type of labeled cells. For simplicity, we will refer to the differently marked clones by color names as displayed in the images. For example, a clone marked only by the expression of β-galactosidase (β-gal) will be called blue; a clone marked by both GFP and RFP will be called yellow. A short heat-shock is likely to induce relatively few recombination events and mostly results in cells marked by a single-marker (green, red, blue). By contrast, a longer heat shock favors many more recombination events, thereby generating doubly (yellow, teal, purple) and triply marked cells (white) (Fig. 1C; supplementary material Fig. S1A-F). Intermediate heat-shock times can produce tissues with all seven classes of cells represented, as well as 'black' unmarked cells (Fig. 1D-H).

As labeling can occur in cells that are not actively undergoing mitosis, recombination can be induced even under periods of cellular quiescence, as occurs during periods of embryogenesis, or following terminal differentiation. In addition to imaginal discs, we have used the TIE-DYE method in a variety of other tissues, including the larval brain and the adult ovary (supplementary material Fig. S1G,H).

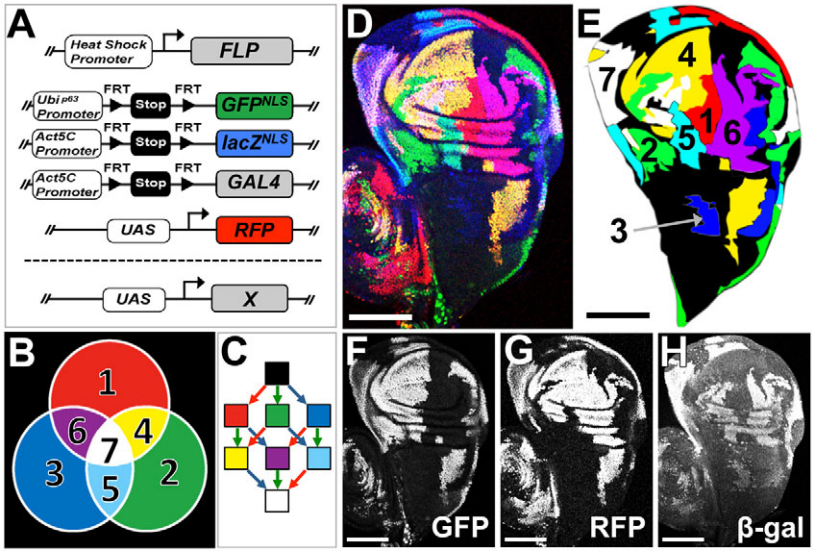

Fig. 1. The *Drosophila* TIE-DYE system. (**A**) Schematic of the TIE-DYE system. (1) The site-specific recombinase (FLP) expressed under the control of the heat-shock promoter; (2) three independent constructs that can activate expression of GFP^{NLS}, $lacZ^{NLS}$ and GAL4 following FRT-mediated recombination; (3) UAS-his2A::RFP to visualize GAL4-expressing cells; and (4) additional UAS-driven constructs that are expressed in GAL4-expressing cells. (**B**) Seven different colors can be generated because of the combinations of activating one, two or all three lineage markers following FLP/FRT-mediated recombination: (1) red, (2) green, (3) blue, (4) yellow, (5) teal, (6) purple and (7) white. (**C**) The recombination events that turn on the expression of markers are irreversible. The color of the arrows (red, green or blue) indicates the recombination event that can produce a given color (squares). (**D**) Wing disc from a 3rd instar larva with all seven colors represented obtained by heat shocking for 30 minutes during late embryogenesis. (**E**) Clone area tracing to emphasize the seven different colors. (**F-H**) The individual channels for the image in D are shown: (F) GFP, (G) UAS-RFP and (H) β-galactosidase. The disc is oriented with anterior towards the left and ventral upwards. Scale bars: 100 μm.

Assessing the clonal composition of discs during normal and compensatory situations

Most tissues, including *Drosophila* imaginal discs, are generated by clonal expansions of relatively small numbers of founder cells. During early embryonic development, multiple cells from two different parasegments are specified to become the wing imaginal disc (reviewed by Serrano and O'Farrell, 1997), and are restricted in fate to either the anterior or posterior compartment (Garcia-Bellido et al., 1973). The wing-imaginal disc primordia invaginate and mostly separate from the rest of the embryonic epithelium between 9 and 11 hours AEL (Bate and Arias, 1991). Soon afterwards, the cells arrest in G_1 for the remainder of embryogenesis (Knoblich et al., 1994). Each compartment of the wing disc is therefore composed of multiple clones of cells and has been described as a 'polyclone' (Crick and Lawrence, 1975). Except for a relatively smooth boundary that separates anterior cells from posterior cells, the clonal boundaries within each compartment are irregular and do not obviously correspond to any anatomical landmark. We used the TIE-DYE system to study the wing-imaginal disc under normal and compensatory growth conditions to address two questions: (1) how many founder cells in a late stage embryo normally contribute to the wing-imaginal disc?; and (2) from this invaginated primordium, what is the smallest number of cells that can generate a wing-imaginal disc?

Previous studies estimate that 38-50 cells give rise to the wing-imaginal disc. These estimates were made by counting the cells in the late-stage embryo (Madhavan and Schneiderman, 1977) or by taking the reciprocal of the fraction of the area of the adult wing that is covered by a single large clone (Garcia-Bellido and Merriam, 1971). We wanted to take advantage of having seven uniquely labeled, plus one unlabeled, cell populations to estimate the number of founder cells present in the late stage embryo. Simply counting the number of labeled patches (marked + unmarked) in the wing disc, would underestimate the number of founder cells, because some of those patches could be composed of more than one clone. If two adjacent clones were to express the same combination of markers, they would form a single contiguous patch. To prevent clones of the same color from touching, one could generate very rare clones by using a short heat-shock; however, this would generate very few labeled clones and leave large portions of the disc unlabeled.

We have developed an alternative method for estimating the number of founder cells that is based on the probability of having each class of clones represented in the disc. As each transgene has a specific probability of being activated by a given heat shock, the probability of all eight classes (each of the seven colors and black) being represented in any single disc increases as the number of founder cells increases. For example, if the wing disc derives from a single founder cell, then the whole disc would always express a single combination of markers. If a disc derives from three founder cells, then the maximum number of different colors that could be present would be three (Fig. 2A). If the number of founder cells were extremely large, then all eight classes would be found in most, if not all, discs (for a heat shock of the appropriate duration).

We generated a simple mathematical model to determine the likely number of founder cells, in a late-stage embryo, that gives rise to the wing imaginal discs, under normal and stressed (irradiated) conditions. An estimated recombination frequency of each of the three constructs (GFP, GAL4, *lacZ*) was determined by measuring the fraction of area in 3rd instar discs that have flipped a given construct (supplementary material Fig. S2A). The frequencies of clones with multiple FLP-out markers was consistent with each recombination event occurring independently of the

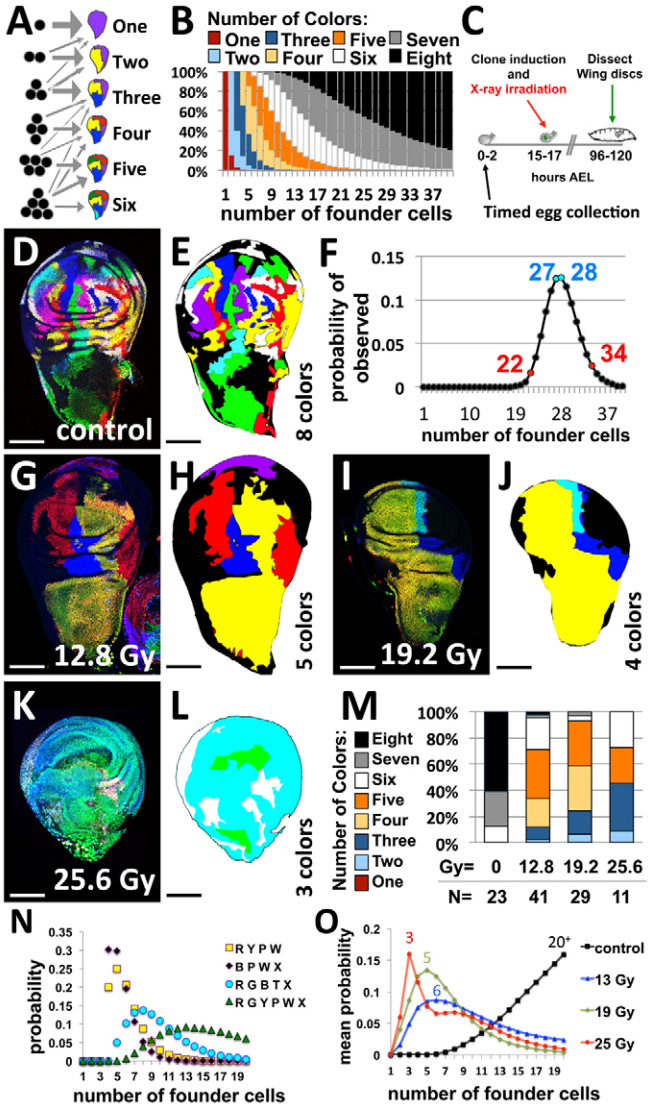

Fig. 2. Modeling the number of expected colors. (A,B) How the number of founder cells, at the time of labeling, affects the number of unique colors present in the resulting tissue. (**A**) A schematic of how the number of founder cells, represented as black circles, affects the number of colors present in that tissue. Examples from one founder cell through eight founders are shown where the weight of the arrow is an indication of the likelihood of that many colors generated, ranging from 1-8 colors (including 'black'). (**B**) The number of expected colors, shown as a percentage of possible outcomes, in a tissue originating from different numbers of founder cells, at the time of labeling. (**C**) Schematic of experiments for estimating numbers of founder cells. (**D**,**E**) Control (D) non-irradiated wing disc and (E) clone area tracing. (**F**) The probability distribution for how many founder cells (from 1-40) best explain the colors present in control (non-irradiated) discs (*n*=23). Blue numbers label peak and red numbers indicate range of >95% confidence interval. (**G-L**) X-ray-irradiated animals that received (G,H) 12.8 Gy, (I,J) 19.2 Gy or (K,L) 25.6 Gy of radiation. (**M**) Summary of the number of colors present in all wing imaginal discs analyzed for the given conditions. 0 Gy=control. *N*=number of wing discs. (**N**) The probability that a subset of specific colors in a disc arose from a given number of founder cells. The key shows examples with particular colors present (R, red; Y, yellow; G, green; T, teal; B, blue; P, purple, W, white; X, black). (**O**) The mean probability for a tissue to have arisen from 1-20 founder cells for the particular color combinations observed in the experimental tissues. The numbers written on the graph indicate the peak for each condition. Scale bars: 100 μm.

others (supplementary material Fig. S2B), suggesting that multiply marked clones are not predisposed to death because of chromosomal rearrangements. For a heat-shock of 30 minutes at 16±1 hours AEL, the average recombination frequencies were calculated to be Act < <GAL4=0.50, Ubi < <GFP=0.49 and Act < <*lacZ*=0.28, which were used to calculate the probability of each color (see Materials and methods). From these frequencies of each color, the model estimates the likelihood of each possible color combination for 1-40 founder cells. As the founder cell number increases, as expected, the likelihood of generating a disc with seven or eight colors increases, and the likelihood of generating a disc with only three or four colors significantly decreases (Fig. 2A,B). Similar curves are generated even when recombination frequencies are a standard deviation above or below the average (supplementary material Fig. S2C). The background (without heat shock) recombination frequency in the wing imaginal disc was low; we observed single clones in ~7% of wing discs (n=82). A higher frequency (~30%) was observed for the myoblasts associated with the wing disc. We would not expect this ~7% background frequency to have a large effect on our estimates as it would only impact our calculations if this additional recombination event generated a color that was not already present in the disc. However, it could increase the number of different colors of clones present slightly and result in a small overestimation of the number of founders. In addition, the background recombination frequency was not elevated by X-ray irradiation (one disc had a single clone, n=25).

TIE-DYE clones were induced in late-stage embryos at 16±1 hours AEL; for the X-ray irradiation experiments, the embryos were irradiated shortly after clone induction, which is expected to eliminate some of the precursor cells (Fig. 2C). The disc precursor cells that survive the X-ray irradiation would then generate the entire wing imaginal disc. Irradiation would be expected to generate a tissue with fewer and larger clones than normal.

We used our model to estimate the number of precursor cells at a late stage of embryogenesis that contribute to the disc proper (excluding the peripodial epithelium) of the 3rd-instar wing-imaginal disc. A wild-type (non-irradiated) wing imaginal disc is shown in a merged image (Fig. 2D) and a clone area tracing of the differently labeled clones present in the disc proper (Fig. 2E). All possible marked and unmarked clone types (eight in total) are present in this disc, as was seen in 61% of the discs (n=23). In addition, 26% discs contain seven classes and 13% discs contain six classes. Based on the relative probabilities of obtaining specific color combinations from different numbers of founder cells (1-40), we calculated the number of founder cells that would best explain the observed discs (Fig. 2F). The model predicts with >95% confidence interval that the disc is derived from 22-34 precursor cells. This prediction can be refined further with lower levels of confidence to 25-31 founders (~73% confidence). This is lower than the estimate of 38 founder cells derived by counting the number of cells in the wing imaginal primordium of 1st instar larvae (Madhavan and Schneiderman, 1977). This may be because not all cells in the morphologically recognizable primordium contribute to the disc proper of the wing imaginal disc. Martín et al. (Martín et al., 2009) recently estimated that the disc proper region of the mature larval wing disc is composed of ~30,000 cells. Based on measured doubling times at different stages of development, they calculated that cells undergo an average of 9.1 doublings, which results in an estimate of 55 founder cells. Our estimate of 22-34 founders would be predicted to generate 30,000 cells if there were, on average, slightly more than 10 cell divisions.

We next examined the effect of reducing the number of founder cells by X-ray irradiation on the number of different classes of discs (e.g. discs with four colors, five colors, etc.). First, we determined how sensitive the cells of the imaginal disc primordium (at 16±1 hours AEL) were to X-ray irradiation. As the dose of X-ray irradiation increased, the number of viable adults decreased and so did the presence of recognizable imaginal discs (supplementary material Fig. S3A,B). At an X-ray dose of 32 Gy, too few precursors cells survived to generate a wing disc. As embryos were subjected to increasing doses of X-ray irradiation, fewer discs of normal size and shape were observed and in these there was a shift towards classes of discs that had relatively few large clones and few classes of marker expression. Merged images and clone area tracing of the discs for increasing doses of X-ray irradiation: 12.8 Gy (Fig. 2G,H), 19.2 Gy (Fig. 2I,J) and 25.6 Gy (Fig. 2K,L). The number of colors present in the disc proper for each experimental condition is summarized in Fig. 2M. At a low dose of irradiation (12.8 Gy), the majority of larvae still had both wing imaginal discs, but there was limited adult viability (~17%). At higher X-ray irradiation doses of 19.2 Gy and 25.6 Gy, ~20-50% of wing discs were absent. Some of the recovered wing discs looked morphologically normal (supplementary material Fig. S3C,D), whereas others were of abnormal shape (supplementary material Fig. S3E,F). At 25.6 Gy of irradiation, the most frequent class of discs was one that only

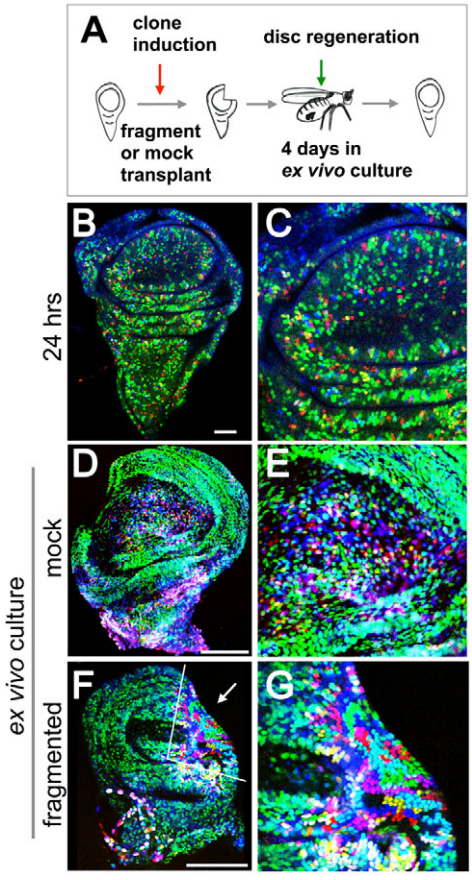

Fig. 3. Imaginal disc regeneration in *ex vivo* culture. (**A**) Schematic of experimental design. TIE-DYE clones were induced in 3rd-instar larvae. (**B**,**C**) Control, without *ex vivo* culture, 24 hours after clone induction. (**D**,**E**) Non-fragmented control cultured *ex vivo*. (**F**,**G**) Fragmented wing disc cultured *ex vivo*. The two white lines indicate the approximate cut sites. The arrow indicates the area of regeneration. Note the larger areas of a single color in G compared with the salt-and-pepper pattern of cell labeling in C and E. Scale bars: 100 μm.

contained three different colors (Fig. 2M). The particular classes of colors observed in the discs recovered from the irradiated embryos were used to calculate the probability of the disc originating from 1-20 founder cells. Example probabilities are shown in Fig. 2N. For a disc that consists of only red, yellow, purple and white regions, the model predicts that there is a ~25% chance that it originated from five founder cells and approximately equal chances that it originated from four or six founder cells (~20%). In addition, the model predicts that there is a 95% probability that this disc originated from between four and nine cells. A disc that consists only of blue, purple, white and black has a 95% probability that it originated from four to seven cells. As there is expected to be considerable variation in the number of founder cells following irradiation, we did not attempt to fit all the data to a single number of founder cells for each dose of irradiation. If all the data were fitted to a single number of founder cells, finding a single disc with six colors would result in zero probability of generating a disc from four founder cells. Instead, for each disc we calculated the probability that it could arise from each number of founder cells in the range of 1-20 cells. We then present, the 'average curve' for each dose of irradiation (Fig. 2O). Thus, increasing doses of X-irradiation reduce the number of founder cells that can still generate a disc of normal size. Moreover, we have observed multiple instances of discs that are likely to have derived from as few as two to four founder cells, which is ~1/8th-1/16th the number found in normal embryos. Assuming an exponential increase in cell number, these founder cells are predicted to have undergone three or four rounds of additional cell proliferation to generate a disc of normal size and shape.

Visualizing regenerative growth with TIE-DYE

Regeneration in *Drosophila* imaginal discs can be observed either by damage *in situ* (Smith-Bolton et al., 2009; Bergantiños et al., 2010) or by culturing fragmented discs in the abdomens of adult females (Hadorn et al., 1949; reviewed by Worley et al., 2012). Imaginal discs regenerate by forming a blastema, which is an area of localized proliferation. The Twin-Spot Generator (Griffin et al., 2009) was used in fragmented eye-antenna discs undergoing transdetermination to show that relatively few cells generated the transdetermined tissue (Sustar et al., 2011). We used TIE-DYE to visualize regenerative growth after physical damage to the imaginal disc (Fig. 3A). TIE-DYE clones were induced in 3rd instar larvae. By this stage of development, most cells accumulate in G2 and then undergo two additional rounds of mitosis during the pupal stage of development (Fain and Stevens, 1982; Graves and Schubiger, 1982; Milán et al., 1996; Neufeld et al., 1998). Thus, in undamaged larval imaginal discs recovered 24 hours after mid-3rd instar clone induction, individual cells express different combinations of the three markers and the disc overall has a 'salt-and-pepper' pattern of different colors (Fig. 3B,C). To trigger regenerative growth, discs lacking a region from the ventral part of the disc were implanted into the abdomens of adult female flies (see Materials and methods) (Fig. 3A). Discs that were implanted without fragmentation looked similar to discs that had not been transplanted (Fig. 3D,E). However, the damaged discs had several clones, each composed of many cells in the part of the disc where tissue had been removed (Fig. 3F,G). Discs from 3rd instar larvae consistently have a much higher frequency of recombination for the Ubi <stop <GFP construct, possibly owing to a more accessible chromatin state for this transgene. Thus, the recombination frequencies of the different constructs seem to be dependent on developmental stage and the type of tissue.

Visualizing cell-autonomous effects on growth

The TIE-DYE system potentially allows for a rapid assessment of the effect of gene overexpression or knockdown on tissue growth in imaginal discs. Conventionally, these experiments are carried out by acquiring images from large numbers of discs in which mutant clones have been generated at low density. Clones are typically compared with their wild-type sister clones generated by mitotic recombination using the MARCM method (Lee et al., 2000) or the twin-spot MARCM (Yu et al., 2009) where GAL4 is expressed in one of the two daughter cells following mitotic recombination.

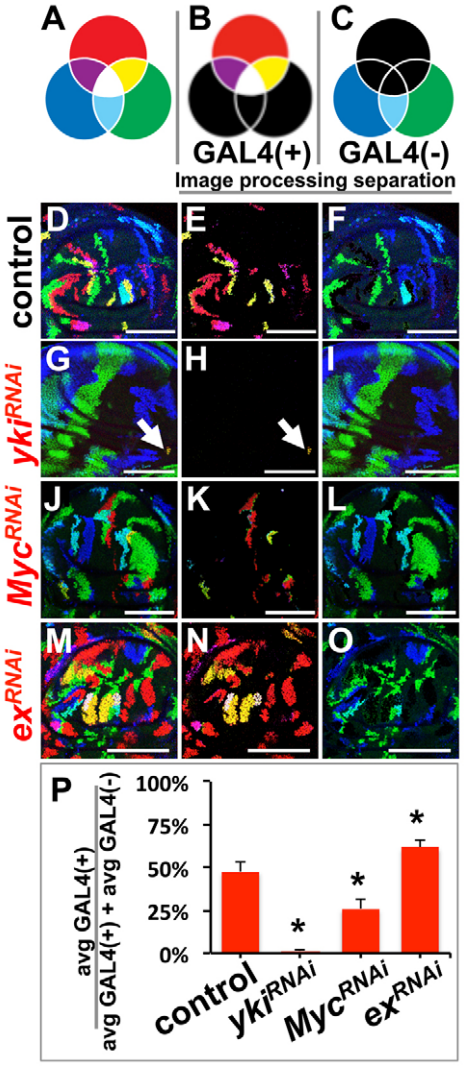

Fig. 4. GAL4-mediated expression of transgenes in a subset of the marked cells shows cell-autonomous changes in growth. (**A-C**) The types of marked clones (A), the subset that are GAL4/UAS dependent (red, yellow, purple and white) (B) and the subset that are do not express GAL4 (blue, teal, green) (C). TIE-DYE clones were induced in the 2nd or early 3rd instar larva. Merged images of 3rd instar wing pouches in the first column; images processed to show only GAL4-expressing clones, in the center column; or clones that do not express GAL4, in the third column. (**D-O**) The GAL4-dependent clones are overexpressing: (D-F) *UAS-dicer2*, (G-I) *UAS-dicer2; UAS-yki*^{RNAi}, (J-L) *UAS-Myc*^{RNAi}*; UAS-dicer2* and (M-O) *UAS-dicer2; UAS-ex*^{RNAi}. (**P**) Percent of average clone area that is GAL4(+) from three separate discs. Quantification of the average GAL4(+) and GAL4(–) clone sizes based on multiple clones from each tissue. See Materials and methods for statistical test (*P<0.01 between experiment and control). Scale bars: 100 μm.

Alternatively, FLP-out clones that co-express a gene or RNAi construct together with a marker are compared with discs of the same developmental stage that have FLP-out clones expressing only the marker. However, this type of comparison can be complicated by changes in the rate of developmental progression caused by gene overexpression or knockdown.

To determine whether, using TIE-DYE, the effects of overexpression or knockdown can be discerned even from single discs, we crossed the TIE-DYE tester stock to fly stocks bearing transgenes that are predicted to impact tissue growth. All clones expressing UAS-RFP also express a UAS-RNAi transgene and *UAS-dicer2*, whereas clones without RFP do not (Fig. 4A-C). Expression of *UAS-dicer2* (Fig. 4D) was used as a control to show the relative size of the GAL4/UAS clones (Fig. 4E) and GAL4-independent clones (Fig. 4F). Reducing the expression of the growth-promoting genes *yorkie* (*yki*) (Huang et al., 2005) (Fig. 4G-I) and *Myc* (Johnston et al., 1999) (Fig. 4J-L) resulted in a reduction of clone size and frequency, presumably owing to some clones being eliminated from the tissue. Conversely, knockdown of the negative regulator of growth, *expanded* (*ex*) (Boedigheimer and Laughon, 1993), caused a slight increase in clone size (Fig. 4M-O). The data were quantified by averaging the area from multiple GAL4(+) and GAL4(–) clones in the wing pouch from multiple discs. When the areas of labeled clones were measured, the fraction of the area accounted for by GAL4(+) clones is close to 50% in controls and is clearly reduced following the knockdown of *yki* or *Myc* (Fig. 4P), and increased slightly with *ex* knockdown (Fig. 4P; supplementary material Fig. S4). All differences are statistically significant.

Examining disc-wide effects of misexpressing patterning genes

The morphogen Dpp plays a crucial role in patterning of the wing disc through induction of different target genes in a concentration-dependent manner (Affolter and Basler, 2007). Dpp is expressed in a strip of cells anterior to the compartment boundary from where it diffuses both anteriorly and posteriorly to regulate growth and patterning. Overexpression of Dpp can lead to overgrowth and changes in wing patterning (Capdevila and Guerrero, 1994; Tabata et al., 1995; Zecca et al., 1995) in a region-specific manner (Rogulja and Irvine, 2005). Hedgehog (Hh) signaling controls the expression pattern of *dpp*. The posterior compartment produces the ligand Hh whereas only the anterior cells are able to receive the signal. We tested the effect of the knockdown of *cubitus interruptus* (*ci*), a transcriptional regulator of the Hh signaling pathway, and observed substantial overgrowth of one side of the wing disc (Fig. 5A-C). Ci can be a transcriptional activator or, after being processed by the proteasome, a transcriptional repressor (reviewed by Jiang and Hui, 2008). The knockdown of *ci*, which is expressed only in the anterior compartment (Eaton and Kornberg, 1990; Orenic et al., 1990; Schwartz et al., 1995), is predicted to reduce levels of both the activator and repressor forms of Ci. The knockdown of *ci* leads to overgrowth localized to the anterior of the wing-imaginal disc (Fig. 5B), which is likely due to reduced levels of the repressor form of Ci that normally prevents the expression of Hh-target genes such as *dpp* in the anterior compartment.

Ectopic expression of *dpp* leads to overgrowth on both the anterior and posterior sides, especially in the lateral parts of the wing-imaginal disc, when compared with the center of the wing pouch (Fig. 5C-F). The medial region of the disc is composed of many small clones, whereas the lateral regions of the disc contain much larger clones (Fig. 5G,H). Importantly, the effect on clone size is observed equally in clones that express GAL4 and those that do not, thus indicating that the effect is not cell-autonomous (Fig. 5I). Thus, at a single glance, it is possible to observe both the region-specific effects as well as the non-cell-autonomous nature of the phenotype.

Using TIE-DYE to study altered cell affinity and cell sorting

One clear advantage of the TIE-DYE system is the ability to visualize both homotypic and heterotypic clone boundaries. Round

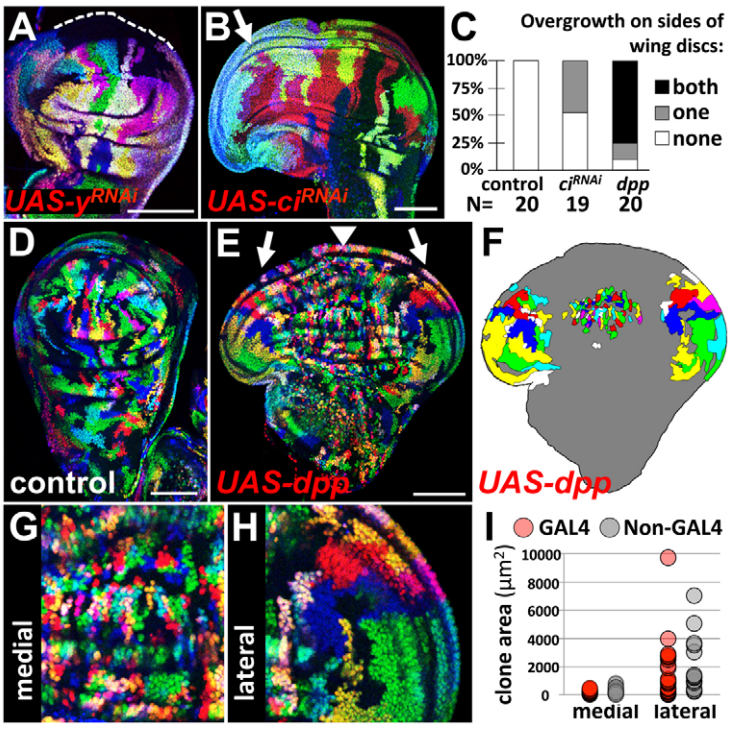

Fig. 5. Region-specific and non-autonomous overgrowth observed using TIE-DYE. (**A**) Wing discs from 3rd instar larvae in which the GAL4(+) cells are expressing an RNAi construct to knockdown *yellow* (*y*) as a control. The dotted line indicates the ventral edge of the disc. (**B**) The RNAi-mediated knockdown of *ci*. There is region-specific overgrowth in the anterior compartment. (**C**) Phenotype of experimental discs with regard to overgrowth on the sides of the disc. (**D**) Control disc, which shows the normal disc morphology and relative clone sizes. (**E**) Wing disc overexpressing *dpp* in the GAL4(+) cells. The arrowhead indicates the medial region of the disc and the arrows indicate the lateral regions. (**F**) Clone tracing to highlight the distinct clone sizes. (**G**,**H**) Higher magnification of the (G) medial and (H) lateral regions. Larger areas of contiguous color are present in the lateral regions when compared with the medial region. (**I**) Measured clone area between the medial and lateral regions. The GAL4(+) and non-GAL4 clones are both larger when located in the lateral region than in the medial region. Scale bars: 100 µm.

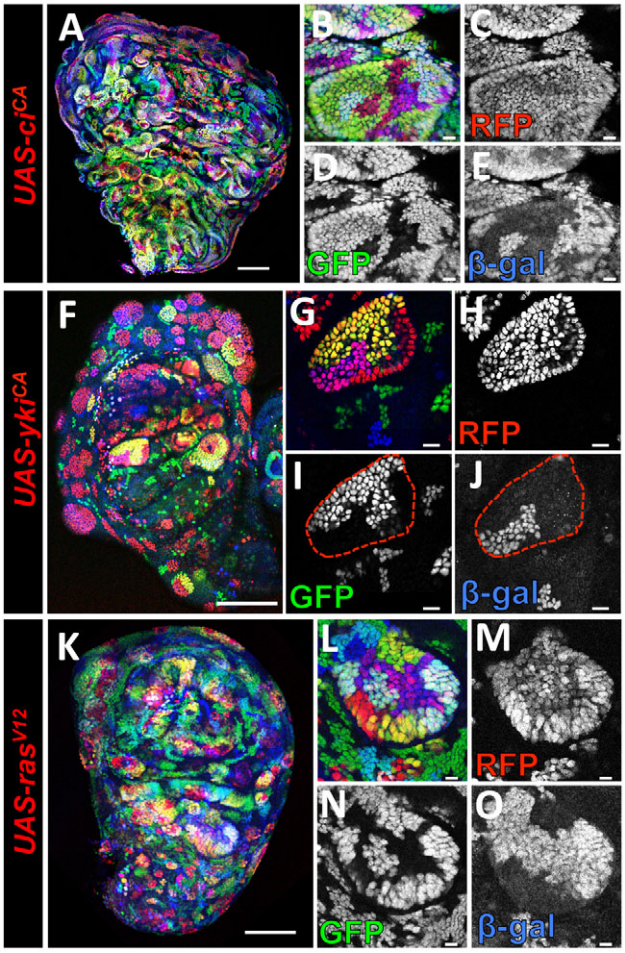

Fig. 6. Clone shape changes caused by growth pathway activation. Wing imaginal discs with GAL4(+) clones expressing constitutively active forms of *yki*, *ci* and *ras*. (**A**) Wing disc with *UAS-ci*^{CA} expression in the *UAS-RFP* marked clones. (**B-E**) Higher magnification of a RFP(+) clone, with separate (C) RFP, (D) GFP and (E) β-gal channels. (**F**) Wing disc with *UAS-yki*^{CA} expression. (**G-J**) Higher magnification of a RFP(+) round clone, with separate (H) RFP, (I) GFP and (J) β-gal channels. The red dotted line is outlining the GAL4(+) clone. Note the irregular clonal boundaries between two differently marked *UAS-yki*^{CA} clones (e.g. purple and yellow), and the size of the RFP(+) clone compared with the other clones. (**K**) Wing disc with *UAS-ras*^{V12} expression. (**L-O**) Higher magnification of a RFP(+) round clone, with separate (M) RFP, (N) GFP and (O) β-gal channels. Scale bars: 100 μm in A,F,K; 10 μm in B-E,G-J,L-O.

clones with smooth boundaries are seen in some cases of clonal overgrowth, possibly because of different adhesive properties of the mutant cells and surrounding wild-type cells (Lawrence and Struhl, 1996; Lawrence et al., 1999). In the wing imaginal disc, clones are elongated along the proximodistal axis because of oriented cell divisions. Mutations in genes that regulate planar cell polarity, such as *fat* and *dachsous*, disrupt oriented cell division and also generate rounder clones (Baena-López et al., 2005). Use of the TIE-DYE system allowed us to determine whether the rounded clones observed by expression of activated forms of Yki, Ci or Ras are due to alterations in cell affinity or perturbations in oriented cell division. Unlike conventional FLP-out clones, the TIE-DYE system allows us to visualize boundaries between individual mutant clones. If the mutant cells have a distinct cell affinity that is different from that of wild-type cells, then we would expect that the boundaries that separate mutant clones to be irregular while those that separate them from wild-type clones would be smooth. By contrast, if these clones were round simply because of defects in oriented cell division, we would expect individual mutant clones to be round. Expression of an activated form of the transcription factor Yki^{S168A} (Oh and Irvine, 2009) (Fig. 6A-E), a non-cleavable form of the transcription factor Ci (Price and Kalderon, 1999) (Fig. 6F-J) or a constitutively active form of Ras (Ras85D^{V12}) (Lee et al., 1996) (Fig. 6K-O) causes clonal outgrowths that appear to sort out from the epithelium. For all three genes, we observed that mutant cells from multiple clones aggregate together in a way in which the boundaries between mutant clones are irregular whereas the boundaries between these cells and wild-type cells are smooth. Thus, application of the TIE-DYE system shows clearly that the shape of the GAL4(+) clones is likely due to perturbation in cell affinity or in cell-cell adhesion.

DISCUSSION

We have developed a method, TIE-DYE, which allows the simultaneous visualization of multiple marked clones in *Drosophila* tissues with the ability to express GAL4-driven transgenes in a subset of clones. However, in its current form, TIE-DYE labeling is ubiquitous. The addition of tissue-specific or temperature-sensitive versions of GAL80 could be used to prevent GAL4-driven expression in specific tissues or at specific developmental stages where such expression might be deleterious to the organism. In addition, fluorescent proteins that localize to specific cellular locations (e.g. membranes) could be used for particular applications (e.g. visualizing neuronal processes). Although we have used TIE-DYE mostly in the wing disc, it can be used to study interactions between populations of cells in any tissue, even those that are composed of post-mitotic cells such as neurons. Finally, although the TIE-DYE system was put together for use in *Drosophila*, analogous systems could be used in most multicellular eukaryotes.

Acknowledgements

We thank F. Serras and his lab for teaching L.S. disc transplantation. We thank U. Banerjee, J. Knoblich and G. Struhl for *Drosophila* fly stocks. We thank A. Gerhold for advice and assistance with the X-ray irradiation experiments, N. Ellis for assistance with experiments, and J. Sadler and C. Worley for help with modeling the number of founder cells. We thank L. Pachter and T. Nystul for advice and discussions, along with Hariharan and Bilder lab members. We also thank N. Patel and the students of the Embryology Course at the Marine Biological Laboratory at Woods Hole (2011) for testing out this system. We thank the TRiP at Harvard Medical School for providing transgenic RNAi fly stocks used in this study and the Bloomington Stock Center.

Funding

I.K.H. is funded by the National Institutes of Health (NIH) [R01 GM61672, R01 GM85576]; and by a Research Professor Award from the American Cancer Society [120366-RP-11-078-01-DDC]. Deposited in PMC for release after 12 months.

Competing interests statement

The authors declare no competing financial interests.

Author contributions

M.I.W. designed the TIE-DYE system, developed the mathematical model for estimating the number of founder cells, and designed and conducted all of the experiments presented in Figs 1,2,4-6. The experiments shown in Fig. 3 were designed and conducted jointly with L.S. I.K.H. was involved in the design and interpretation of the experiments. M.I.W. prepared the figures. M.I.W. and I.K.H. wrote the paper.

Supplementary material

Supplementary material available online at
http://dev.biologists.org/lookup/suppl/doi:10.1242/dev.096057/-/DC1

References

Affolter, M. and Basler, K. (2007). The Decapentaplegic morphogen gradient: from pattern formation to growth regulation. *Nat. Rev. Genet.* **8**, 663-674.

Baena-López, L. A., Baonza, A. and García-Bellido, A. (2005). The orientation of cell divisions determines the shape of Drosophila organs. *Curr. Biol.* **15**, 1640-1644.

Bate, M. and Arias, A. M. (1991). The embryonic origin of imaginal discs in Drosophila. *Development* **112**, 755-761.

Bergantiños, C., Corominas, M. and Serras, F. (2010). Cell death-induced regeneration in wing imaginal discs requires JNK signalling. *Development* **137**, 1169-1179.

Boedigheimer, M. and Laughon, A. (1993). Expanded: a gene involved in the control of cell proliferation in imaginal discs. *Development* **118**, 1291-1301.

Bosch, M., Serras, F., Martín-Blanco, E. and Baguñà, J. (2005). JNK signaling pathway required for wound healing in regenerating Drosophila wing imaginal discs. *Dev. Biol.* **280**, 73-86.

Boulina, M., Samarajeewa, H., Baker, J. D., Kim, M. D. and Chiba, A. (2013). Live imaging of multicolor-labeled cells in Drosophila. *Development* **140**, 1605-1613.

Brand, A. H. and Perrimon, N. (1993). Targeted gene expression as a means of altering cell fates and generating dominant phenotypes. *Development* **118**, 401-415.

Capdevila, J. and Guerrero, I. (1994). Targeted expression of the signaling molecule decapentaplegic induces pattern duplications and growth alterations in Drosophila wings. *EMBO J.* **13**, 4459-4468.

Crick, F. H. and Lawrence, P. A. (1975). Compartments and polyclones in insect development. *Science* **189**, 340-347.

del Valle Rodríguez, A., Didiano, D. and Desplan, C. (2012). Power tools for gene expression and clonal analysis in Drosophila. *Nat. Methods* **9**, 47-55.

Eaton, S. and Kornberg, T. B. (1990). Repression of ci-D in posterior compartments of Drosophila by engrailed. *Genes Dev.* **4**, 1068-1077.

Emery, G., Hutterer, A., Berdnik, D., Mayer, B., Wirtz-Peitz, F., Gaitan, M. G. and Knoblich, J. A. (2005). Asymmetric Rab 11 endosomes regulate delta recycling and specify cell fate in the Drosophila nervous system. *Cell* **122**, 763-773.

Evans, C. J., Olson, J. M., Ngo, K. T., Kim, E., Lee, N. E., Kuoy, E., Patananan, A. N., Sitz, D., Tran, P., Do, M. T. et al. (2009). G-TRACE: rapid Gal4-based cell lineage analysis in Drosophila. *Nat. Methods* **6**, 603-605.

Fain, M. J. and Stevens, B. (1982). Alterations in the cell cycle of Drosophila imaginal disc cells precede metamorphosis. *Dev. Biol.* **92**, 247-258.

Fischer, J. A., Giniger, E., Maniatis, T. and Ptashne, M. (1988). GAL4 activates transcription in Drosophila. *Nature* **332**, 853-856.

Garcia-Bellido, A. and Merriam, J. R. (1969). Cell lineage of the imaginal discs in Drosophila gynandromorphs. *J. Exp. Zool.* **170**, 61-75.

Garcia-Bellido, A. and Merriam, J. R. (1971). Parameters of the wing imaginal disc development of Drosophila melanogaster. *Dev. Biol.* **24**, 61-87.

Garcia-Bellido, A., Ripoll, P. and Morata, G. (1973). Developmental compartmentalisation of the wing disk of Drosophila. *Nat. New Biol.* **245**, 251-253.

Golic, K. G. (1991). Site-specific recombination between homologous chromosomes in Drosophila. *Science* **252**, 958-961.

Graves, B. J. and Schubiger, G. (1982). Cell cycle changes during growth and differentiation of imaginal leg discs in Drosophila melanogaster. *Dev. Biol.* **93**, 104-110.

Griffin, R., Sustar, A., Bonvin, M., Binari, R., del Valle Rodriguez, A., Hohl, A. M., Bateman, J. R., Villalta, C., Heffern, E., Grunwald, D. et al. (2009). The twin spot generator for differential Drosophila lineage analysis. *Nat. Methods* **6**, 600-602.

Gupta, V. and Poss, K. D. (2012). Clonally dominant cardiomyocytes direct heart morphogenesis. *Nature* **484**, 479-484.

Hadjieconomou, D., Rotkopf, S., Alexandre, C., Bell, D. M., Dickson, B. J. and Salecker, I. (2011). Flybow: genetic multicolor cell labeling for neural circuit analysis in Drosophila melanogaster. *Nat. Methods* **8**, 260-266.

Hadorn, E., Bertani, G. and Gallera, J. (1949). Regulative capacity and field organization of male genital discs in Drosophila melanogaster. *Wilhelm Roux Arch. Entwickl. Mech. Org.* **144**, 31-70.

Halme, A., Cheng, M. and Hariharan, I. K. (2010). Retinoids regulate a developmental checkpoint for tissue regeneration in Drosophila. *Curr. Biol.* **20**, 458-463.

Hampel, S., Chung, P., McKellar, C. E., Hall, D., Looger, L. L. and Simpson, J. H. (2011). Drosophila Brainbow: a recombinase-based fluorescence labeling technique to subdivide neural expression patterns. *Nat. Methods* **8**, 253-259.

Huang, J., Wu, S., Barrera, J., Matthews, K. and Pan, D. (2005). The Hippo signaling pathway coordinately regulates cell proliferation and apoptosis by inactivating Yorkie, the Drosophila Homolog of YAP. *Cell* **122**, 421-434.

Hussey, R. G., Thompson, W. R. and Calhoun, E. T. (1927). The Influence of X-Rays on the Development of Drosophila Larvae. *Science* **66**, 65-66.

Jiang, J. and Hui, C. C. (2008). Hedgehog signaling in development and cancer. *Dev. Cell* **15**, 801-812.

Johnston, L. A., Prober, D. A., Edgar, B. A., Eisenman, R. N. and Gallant, P. (1999). Drosophila myc regulates cellular growth during development. *Cell* **98**, 779-790.

Knoblich, J. A., Sauer, K., Jones, L., Richardson, H., Saint, R. and Lehner, C. F. (1994). Cyclin E controls S phase progression and its down-regulation during Drosophila embryogenesis is required for the arrest of cell proliferation. *Cell* **77**, 107-120.

Kretzschmar, K. and Watt, F. M. (2012). Lineage tracing. *Cell* **148**, 33-45.

Lai, S. L. and Lee, T. (2006). Genetic mosaic with dual binary transcriptional systems in Drosophila. *Nat. Neurosci.* **9**, 703-709.

Lawrence, P. A. and Struhl, G. (1996). Morphogens, compartments, and pattern: lessons from drosophila? *Cell* **85**, 951-961.

Lawrence, P. A., Casal, J. and Struhl, G. (1999). hedgehog and engrailed: pattern formation and polarity in the Drosophila abdomen. *Development* **126**, 2431-2439.

Le Douarin, N. M. and Barq, G. (1969). [Use of Japanese quail cells as 'biological markers' in experimental embryology]. *C.R. Hebd. Seances Acad. Sci., Ser. D, Sci. Nat.* **269**, 1543-1546.

Lee, T., Feig, L. and Montell, D. J. (1996). Two distinct roles for Ras in a developmentally regulated cell migration. *Development* **122**, 409-418.

Lee, T., Winter, C., Marticke, S. S., Lee, A. and Luo, L. (2000). Essential roles of Drosophila RhoA in the regulation of neuroblast proliferation and dendritic but not axonal morphogenesis. *Neuron* **25**, 307-316.

Livet, J., Weissman, T. A., Kang, H., Draft, R. W., Lu, J., Bennis, R. A., Sanes, J. R. and Lichtman, J. W. (2007). Transgenic strategies for combinatorial expression of fluorescent proteins in the nervous system. *Nature* **450**, 56-62.

Mandaravally Madhavan, M. M. and Schneiderman, H. A. (1977). Histological analysis of the dynamics of growth of imaginal discs and histoblast nests during the larval development of drosophila melanogaster. *Wilhelm Roux's Archives* **183**, 269-305.

Martín, F. A., Herrera, S. C. and Morata, G. (2009). Cell competition, growth and size control in the Drosophila wing imaginal disc. *Development* **136**, 3747-3756.

Milán, M., Campuzano, S. and García-Bellido, A. (1996). Cell cycling and patterned cell proliferation in the Drosophila wing during metamorphosis. *Proc. Natl. Acad. Sci. USA* **93**, 11687-11692.

Neufeld, T. P., de la Cruz, A. F., Johnston, L. A. and Edgar, B. A. (1998). Coordination of growth and cell division in the Drosophila wing. *Cell* **93**, 1183-1193.

Oh, H. and Irvine, K. D. (2009). In vivo analysis of Yorkie phosphorylation sites. *Oncogene* **28**, 1916-1927.

Orenic, T. V., Slusarski, D. C., Kroll, K. L. and Holmgren, R. A. (1990). Cloning and characterization of the segment polarity gene cubitus interruptus Dominant of Drosophila. *Genes Dev.* **4**, 1053-1067.

Pignoni, F. and Zipursky, S. L. (1997). Induction of Drosophila eye development by decapentaplegic. *Development* **124**, 271-278.

Potter, C. J., Tasic, B., Russler, E. V., Liang, L. and Luo, L. (2010). The Q system: a repressible binary system for transgene expression, lineage tracing, and mosaic analysis. *Cell* **141**, 536-548.

Price, M. A. and Kalderon, D. (1999). Proteolysis of cubitus interruptus in Drosophila requires phosphorylation by protein kinase A. *Development* **126**, 4331-4339.

Rogulja, D. and Irvine, K. D. (2005). Regulation of cell proliferation by a morphogen gradient. *Cell* **123**, 449-461.

Schwartz, C., Locke, J., Nishida, C. and Kornberg, T. B. (1995). Analysis of cubitus interruptus regulation in Drosophila embryos and imaginal disks. *Development* **121**, 1625-1635.

Serrano, N. and O'Farrell, P. H. (1997). Limb morphogenesis: connections between patterning and growth. *Curr. Biol.* **7**, R186-R195.

Smith-Bolton, R. K., Worley, M. I., Kanda, H. and Hariharan, I. K. (2009). Regenerative growth in Drosophila imaginal discs is regulated by Wingless and Myc. *Dev. Cell* **16**, 797-809.

Snippert, H. J., van der Flier, L. G., Sato, T., van Es, J. H., van den Born, M., Kroon-Veenboer, C., Barker, N., Klein, A. M., van Rheenen, J., Simons, B. D. et al. (2010). Intestinal crypt homeostasis results from neutral competition between symmetrically dividing Lgr5 stem cells. *Cell* **143**, 134-144.

Staehling-Hampton, K. and Hoffmann, F. M. (1994). Ectopic decapentaplegic in the Drosophila midgut alters the expression of five homeotic genes, dpp, and wingless, causing specific morphological defects. *Dev. Biol.* **164**, 502-512.

Struhl, G. and Basler, K. (1993). Organizing activity of wingless protein in Drosophila. *Cell* **72**, 527-540.

Sturtevant, A. H. (1929). The claret mutant type of Drosophila simulans: a study of chromosome elimination and of cell-lineage. *Z. Wiss. Zool.* **135**, 323-356.

Sustar, A., Bonvin, M., Schubiger, M. and Schubiger, G. (2011). Drosophila twin spot clones reveal cell division dynamics in regenerating imaginal discs. *Dev. Biol.* **356**, 576-587.

Szüts, D. and Bienz, M. (2000). LexA chimeras reveal the function of Drosophila Fos as a context-dependent transcriptional activator. *Proc. Natl. Acad. Sci. USA* **97**, 5351-5356.

Tabata, T., Schwartz, C., Gustavson, E., Ali, Z. and Kornberg, T. B. (1995). Creating a Drosophila wing de novo, the role of engrailed, and the compartment border hypothesis. *Development* **121**, 3359-3369.
Weisblat, D. A., Sawyer, R. T. and Stent, G. S. (1978). Cell lineage analysis by intracellular injection of a tracer enzyme. *Science* **202**, 1295-1298.
Worley, M. I., Setiawan, L. and Hariharan, I. K. (2012). Regeneration and transdetermination in Drosophila imaginal discs. *Annu. Rev. Genet.* **46**, 289-310.
Xu, T. and Rubin, G. M. (1993). Analysis of genetic mosaics in developing and adult Drosophila tissues. *Development* **117**, 1223-1237.
Yagi, R., Mayer, F. and Basler, K. (2010). Refined LexA transactivators and their use in combination with the Drosophila Gal4 system. *Proc. Natl. Acad. Sci. USA* **107**, 16166-16171.
Yu, H. H., Chen, C. H., Shi, L., Huang, Y. and Lee, T. (2009). Twin-spot MARCM to reveal the developmental origin and identity of neurons. *Nat. Neurosci.* **12**, 947-953.
Zecca, M., Basler, K. and Struhl, G. (1995). Sequential organizing activities of engrailed, hedgehog and decapentaplegic in the Drosophila wing. *Development* **121**, 2265-2278.

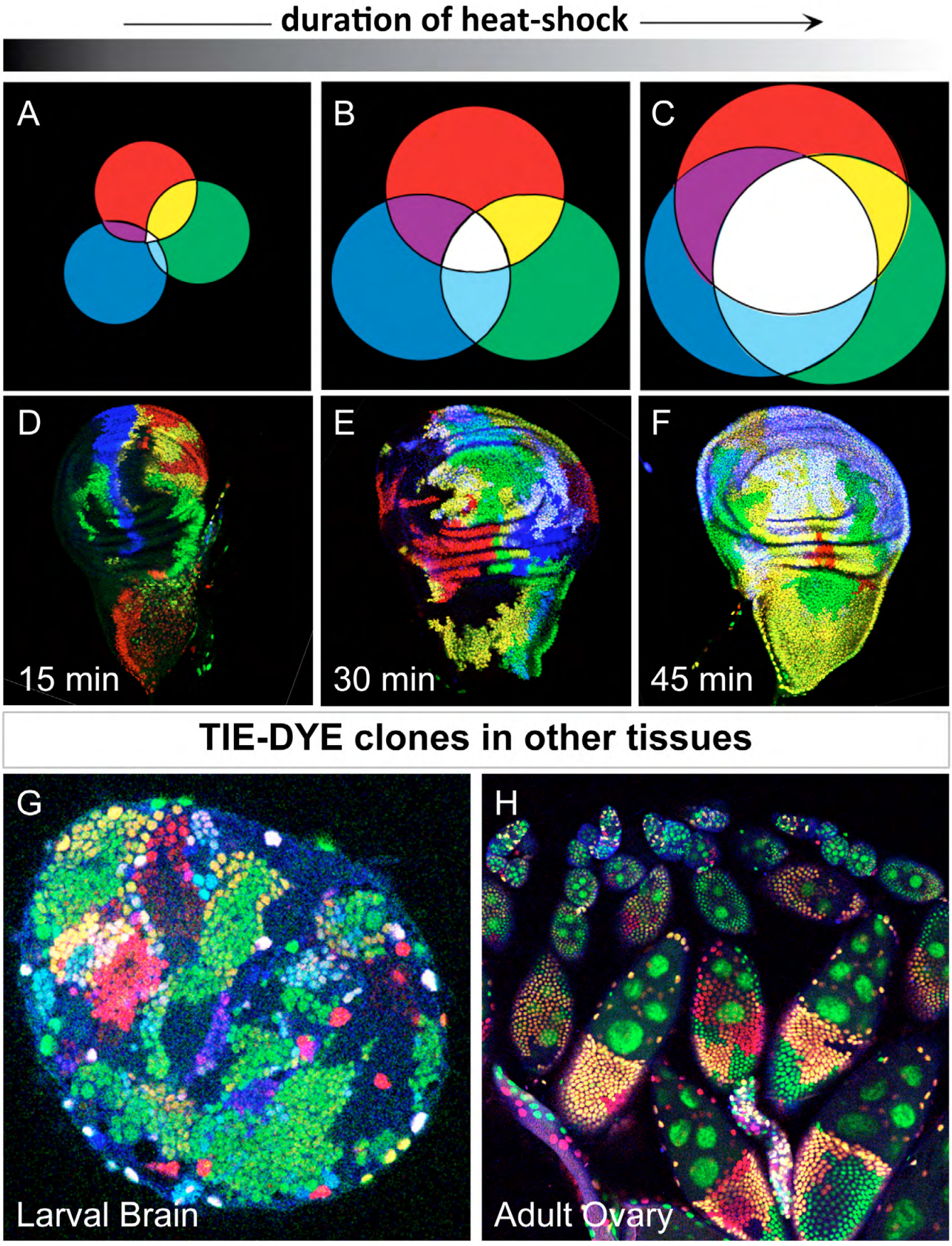

Fig S1. The *Drosophila* TIE-DYE system (**A-F**) The duration of the heat-shock effects the number of cells that are marked by one, two or three of the independent flip-out constructs. (A-C) With a longer heat shock, the proportion of cells are doubly (yellow, teal, purple) or triply labeled (white) increases. (D-F) Third instar wing imaginal discs from animals that were heat-shocked for (D)15, (E) 30 or (F) 45 minutes at 24±2 AEL. There are more yellow and white clones with longer heat shocks. (**G**,**H**) The TIE-DYE method has been tested for generating all the different colors in other tissues, including (G) the larval brain and (H) the adult ovary. *UAS-his2A::RFP* is not expressed in the germ line (because it is not a UASp construct); therefore, the germ line cells only appear green, blue or teal.

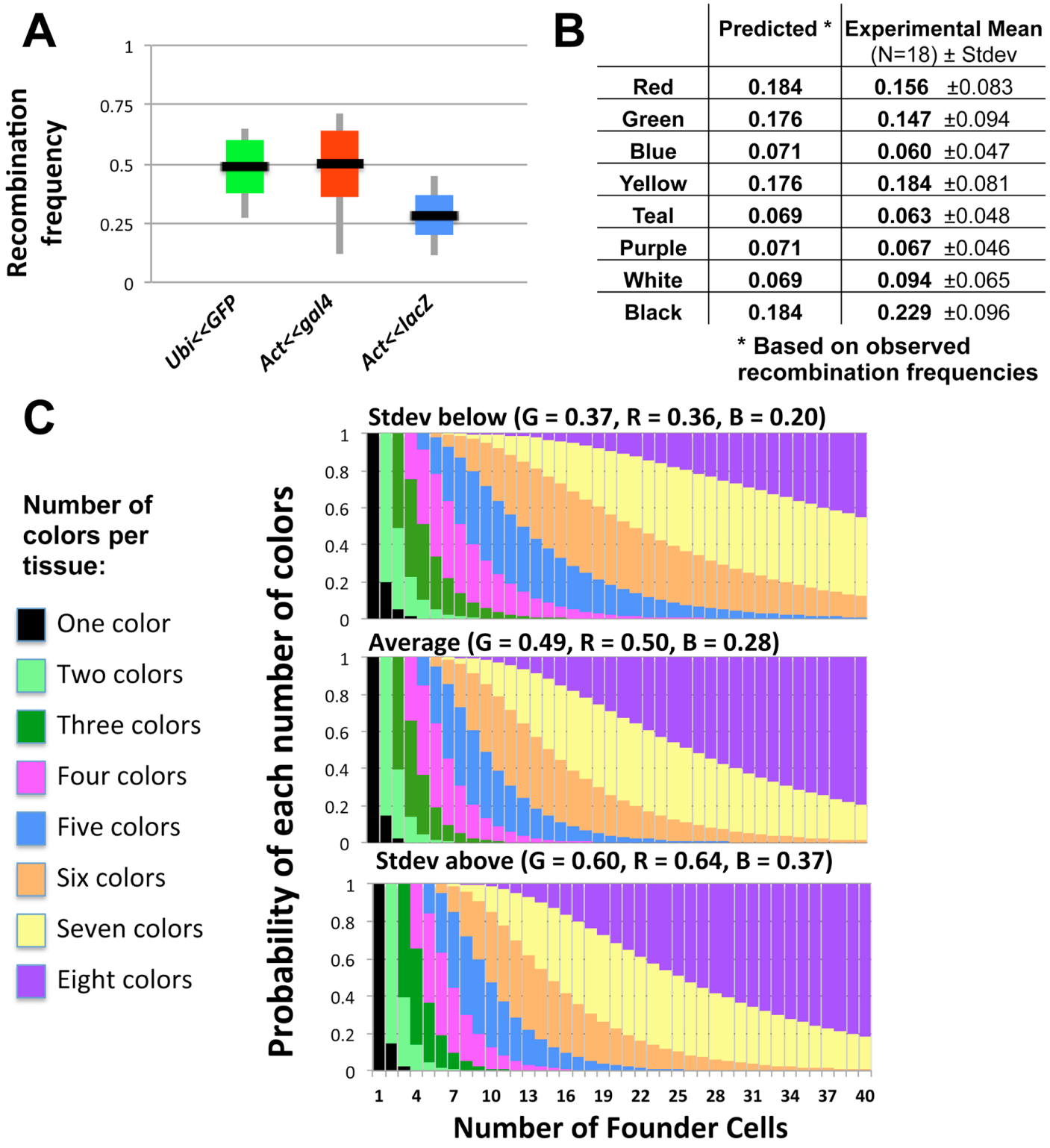

Fig. S2. Modeling the number of colors in a tissue versus the number of founder cells. (**A**) Experimentally calculated recombination frequencies for a 30-minute heat shock at 16±1 hours AEL under non-irradiated conditions. The frequencies were based on the ratio of the area of GFP, RFP and β-gal-positive tissue to total area in third instar wing discs. The black bars show the average (mean), the colored rectangles show a s.d. above and below the mean, and the vertical gray lines show the extremes (*n*=18 discs). (**B**) The predicted versus experimentally observed color frequencies, which are generated by unique marker combinations from the three FLP-out cassettes. The predicted color frequencies were generated using equations that assume the FLP-out events occur independently (see Materials and methods). The predicted color frequencies are all within a s.d. of the experimental color frequencies. (**C**) The modeling of the number of colors predicted to be in a disc based on the number of founder cells using three recombination frequencies (listed above the graphs: G = *Ubi<<GFP*, R = *Act<<GAL4*, *UAS-RFP* and B = *Act << lacZ*). The upper graph represents the model generated with the recombination frequencies a standard deviation below average; the lower graph a standard deviation above the mean. The center graph shows a representation of the model generated by the average recombination frequency (also shown in Fig. 2B) for comparison.

A

IR Dose	% Viable*
12.8 Gy	17 % (N = 183)
19.2 Gy	0 % (N = 183)
25.6 Gy	0 % (N = 97)

*adults

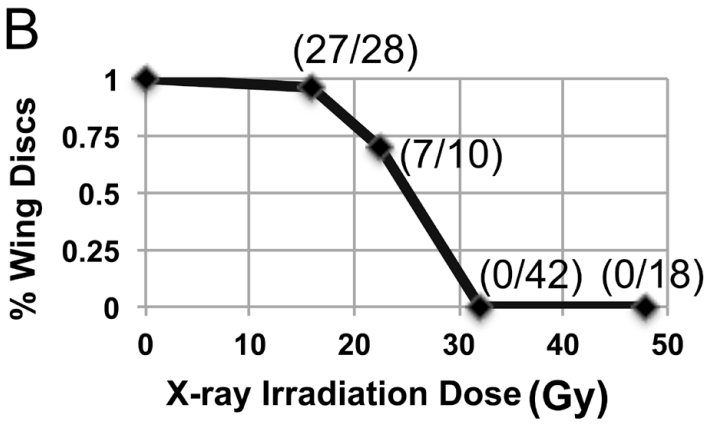

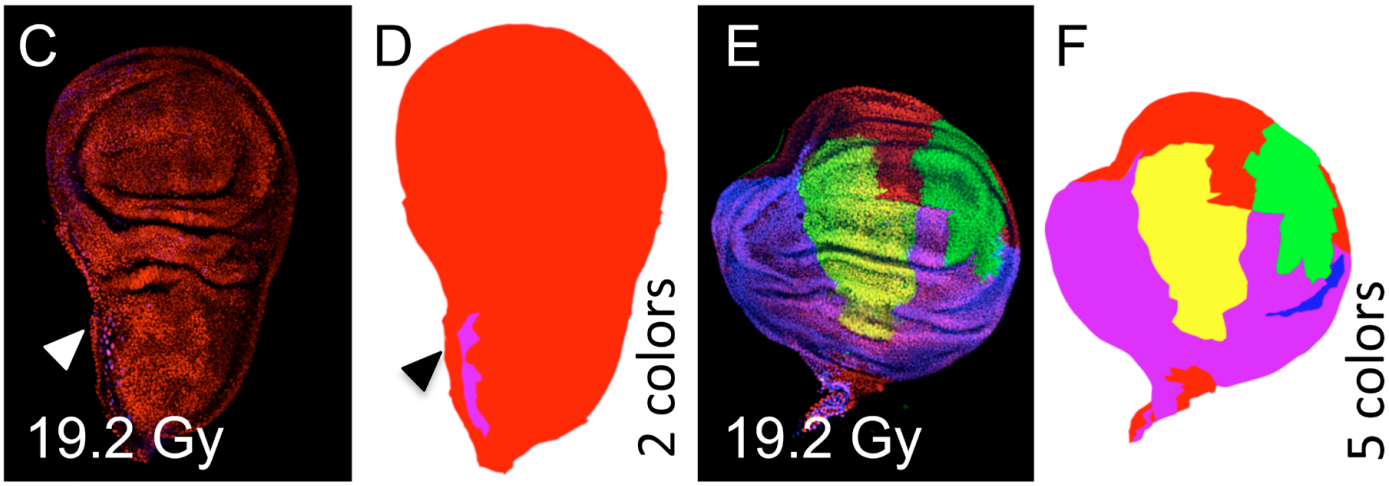

Fig. S3. Additional information on the X-ray irradiation experiments. (**A**) The number of animals that eclosed from their pupal cases compared with the total number of pupal cases observed at different doses of X-ray irradiation. Animals survived to adulthood only with the lowest dose of irradiation. (**B**) The number of wing discs recovered during dissection of third instar larvae at different doses of X-ray irradiation at 16±1 hours AEL. Higher X-ray dose produced larvae without any recognizable imaginal discs. (**C-F**) Additional examples of wing imaginal discs from the intermediate X-ray dose of 19.2 Gy, where C and D show an example of a morphologically normal wing disc that is only made up of two colors, and E and F show an example of a disc with abnormal morphology, with lost or underdeveloped notum, made up of five colors.

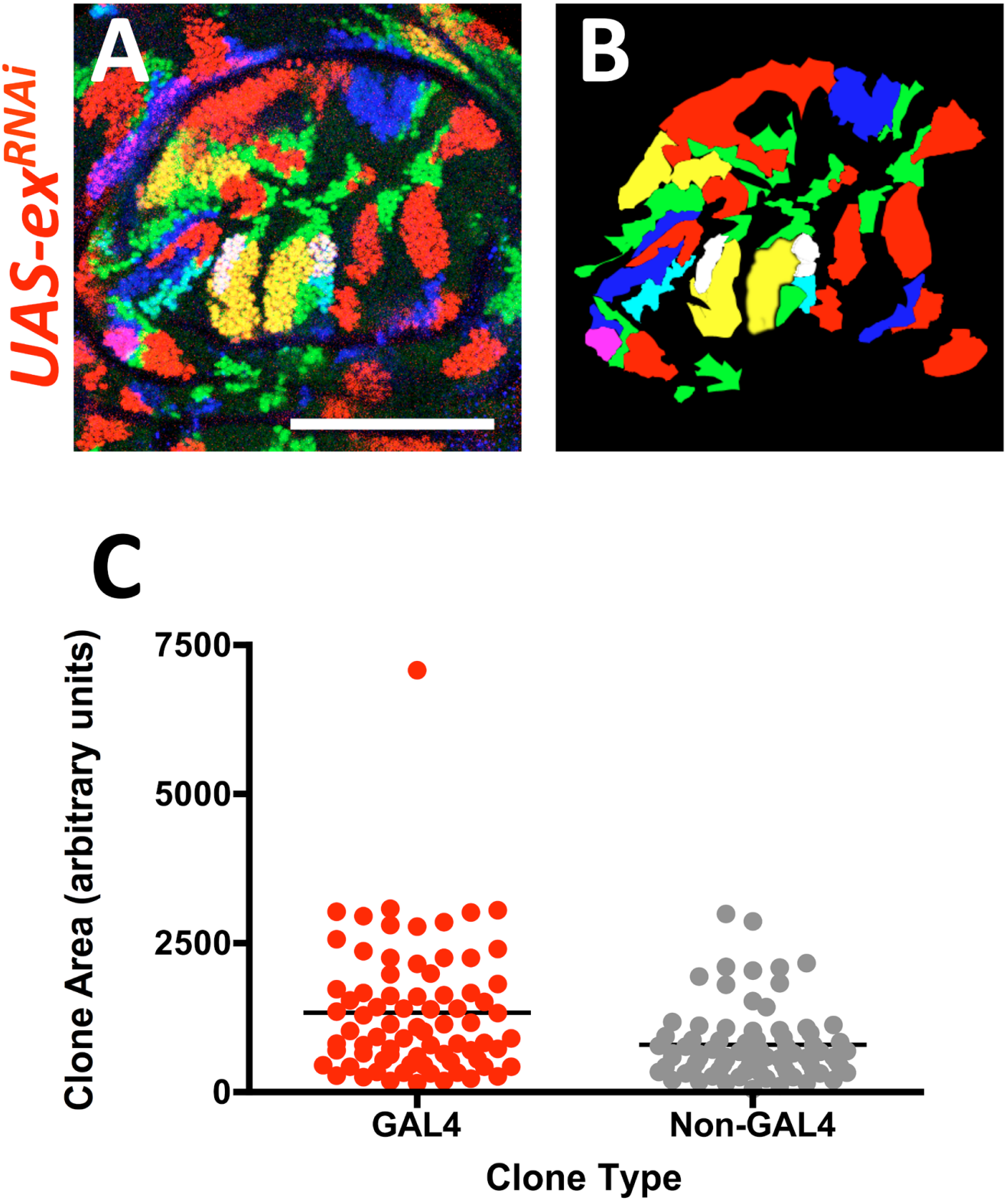

Fig. S4. GAL4(+) clone expressing *UAS-ex*^{RNAi} versus GAL4(–) clone sizes. (**A**) Example of wing pouch expressing RNAi to *ex* (same image as in Fig. 4). (**B**) The clone area tracing to show different color clones. (**C**) The clone area was measured for GAL4 and non-GAL4 clones from three separate wing discs. GAL4(+) clones include red, yellow, purple and white clones. Non-GAL4 clones include blue, green and teal. Each dot is the area of a single clone. The population of GAL4(+) clones are larger than the population of non-GAL4 clones. This difference is statistically significant as assessed by the Mann Whitney test, two-tailed (P=0.0003).